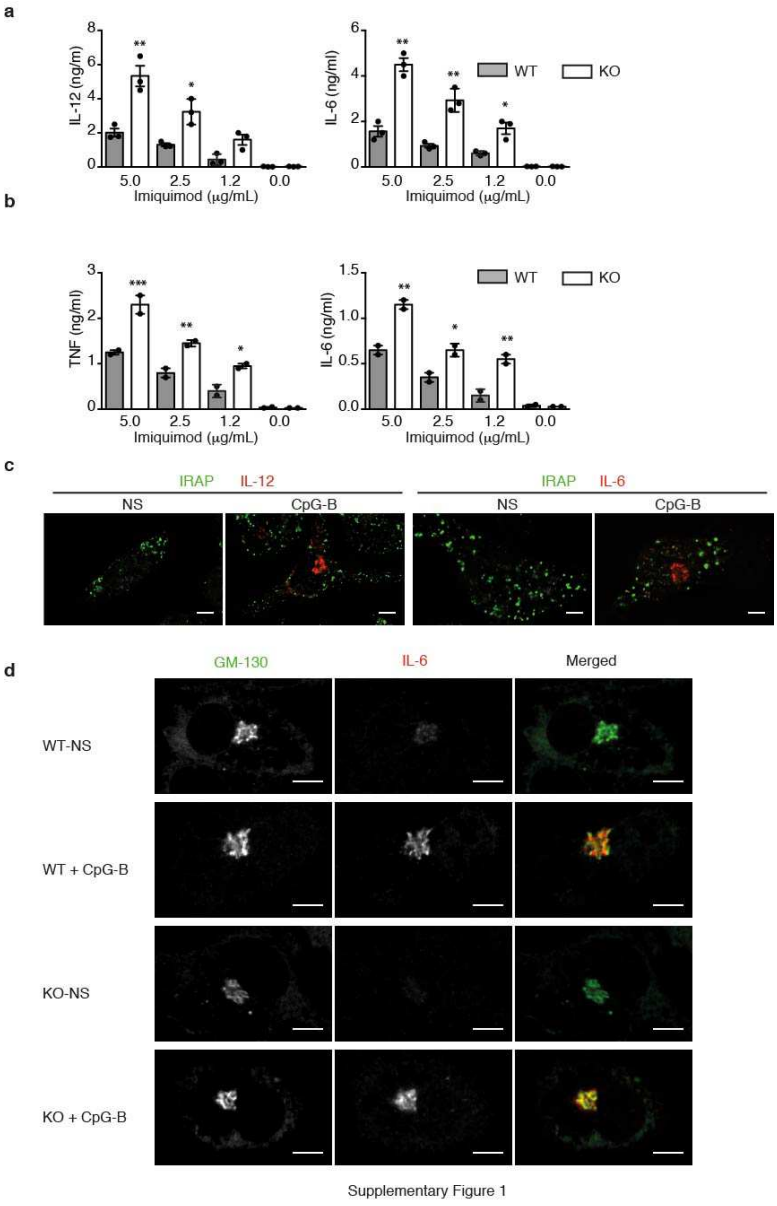

Supplementary Figure 1

Supplementary Figure 1

IRAP-deficient BMDCs have an increased TLR7 response and a normal trafficking of proinflammatory cytokines

(**a-b**) WT and KO BMDCs or splenic pDCs were stimulated with TLR7 ligand (imiquimod) and the secretion of IL-6, IL-12(p40) and TNF was measured by ELISA. (n=3 experiments, mean ± SEM, *p<0.031, **p<0.007,***p<0.0012).
(**c-d**) Immunofluorescence microscopy of BMDCs from WT or KO mice stimulated or not (NS) with CpG-B for 6 hours and stained for IRAP and IL-6 or IL-12(p40) (**a**), and IRAP and GM-130 (**b**) using specific antibodies. Quantification of colocalization showed that 70% (+/-5%) and 80% (+/-7) of IL-6 is found in Golgi stacks in WT and KO cells, respectively (n=10 cells, mean+/-SEM).

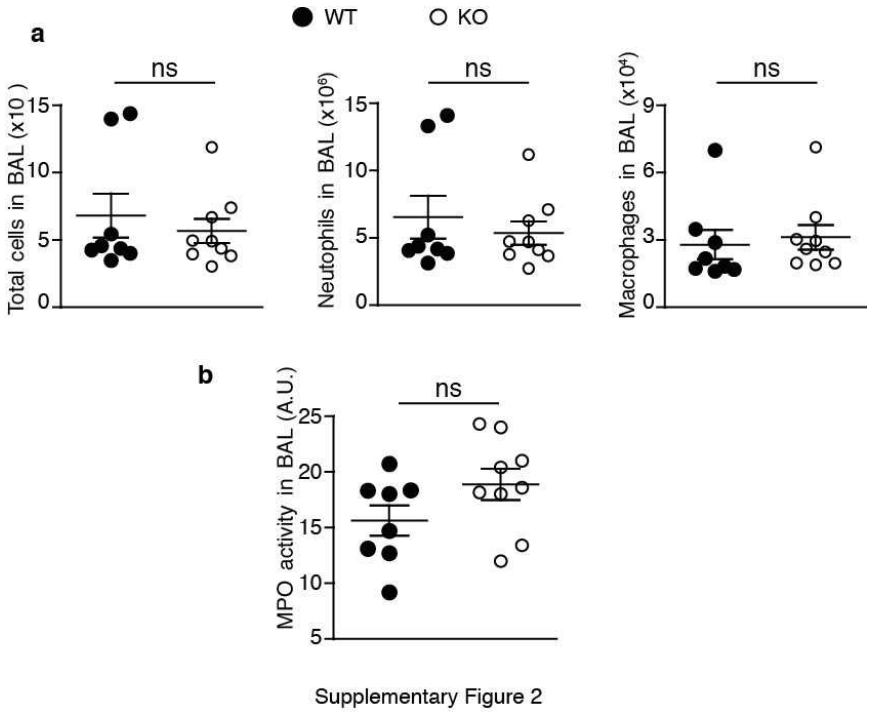

Supplementary Figure 2

The innate inflammatory infiltrate of *Pseudomonas aeruginosa*-infected lungs is not altered by the absence of IRAP

(**a**) The presence of macrophages/monocytes ($CD11b^{+}/GR\text{-}1^{Int}$) and neutrophils ($CD11b^{+}/GR\text{-}1^{high}$) was analyzed by flow cytometry of single cell suspensions in BAL fluids from WT and KO mice 24 h post infection (n=8 animals; mean ± SEM). (**b**) Myeloperoxidase (MPO) activity (lower panel) was measured in BAL fluids from WT and KO mice 24 h post infection (n=8 animals; mean ± SEM).

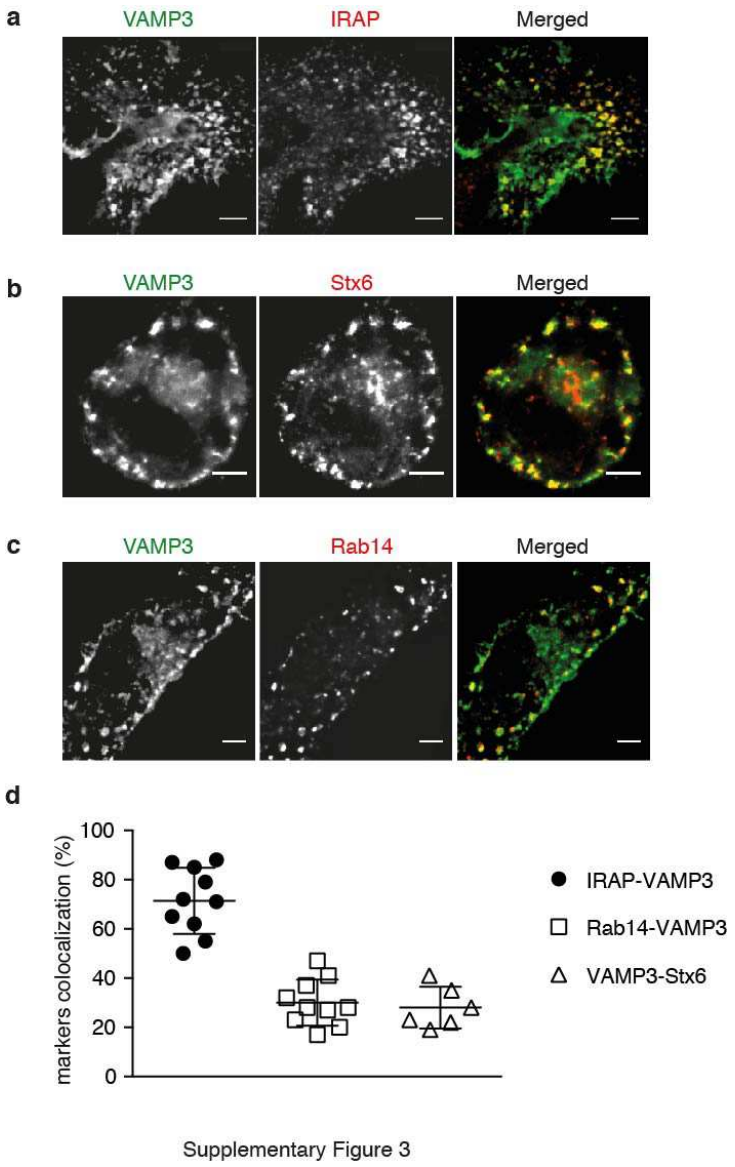

Supplementary Figure 3

Supplementary Figure 3

STX6 and VAMP3 are components of IRAP endosomes

WT BMDCs were transfected with VAMP3-GFP by nucleofection. Two days later, the cells were stained with the antibodies specific for IRAP (**a**), STX6 (**b**) or Rab14 (**c**) and analyzed by confocal microscopy. (**d**) Quantification of colocalization between the two markers (n=10 cells,mean ± SEM).

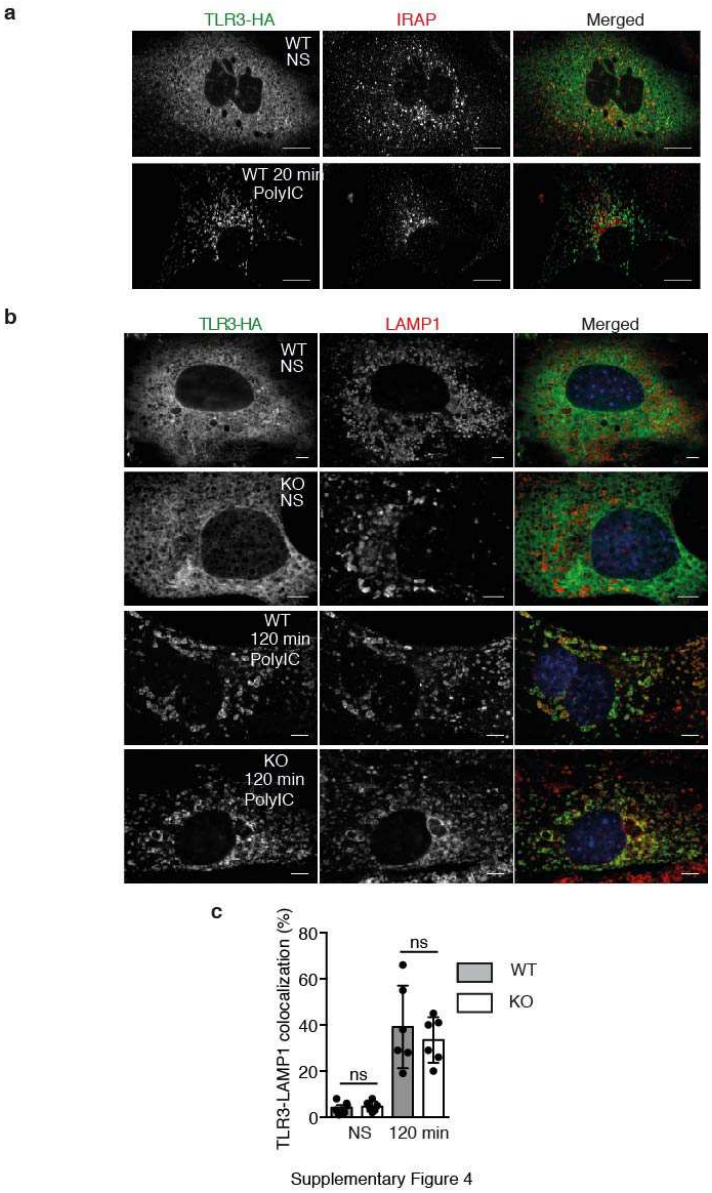

Supplementary Figure 4

TLR3 trafficking is not affected by IRAP deletion

(**a-b**) WT BMDCs were transfected with TLR3-HA by nucleofection. Two days later the cells were stimulated or not (NS) with polyIC for indicated time points, fixed and stained with antibodies against IRAP (**a**) or LAMP1 (**b**). (**c**) Quantification of TLR3-HA and LAMP1 co-localization in the experiment shown in (**b**) using Image J Software (n=10 cells from 2 independent experiments, mean ± SEM).

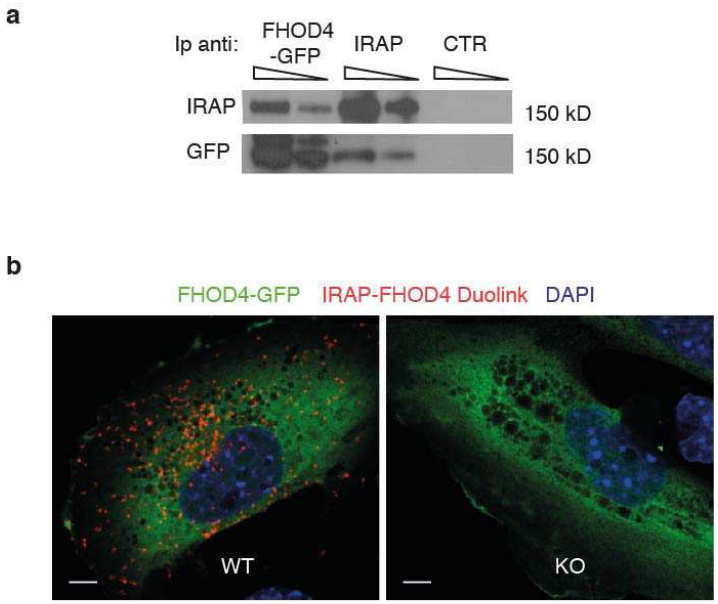

Supplementary Figure 5

Supplementary Figure 5

IRAP interaction with FHOD4 can be reconstituted in wt fibroblasts

(**a**) WT fibroblasts were transfected by electroporation with a plasmid expressing FHOD4-GFP. Thirty-six hours later IRAP and FHOD4 were immunoprecipitated with anti-IRAP and anti-GFP respectively and the precipitates were split in two and analyzed by immunoblot as indicated. (**b**) WT and KO fibroblasts were transfected as in (**a**) and a proximity ligation assay for detection of IRAP/FHOD4 interaction was performed with antibodies against IRAP and GFP.

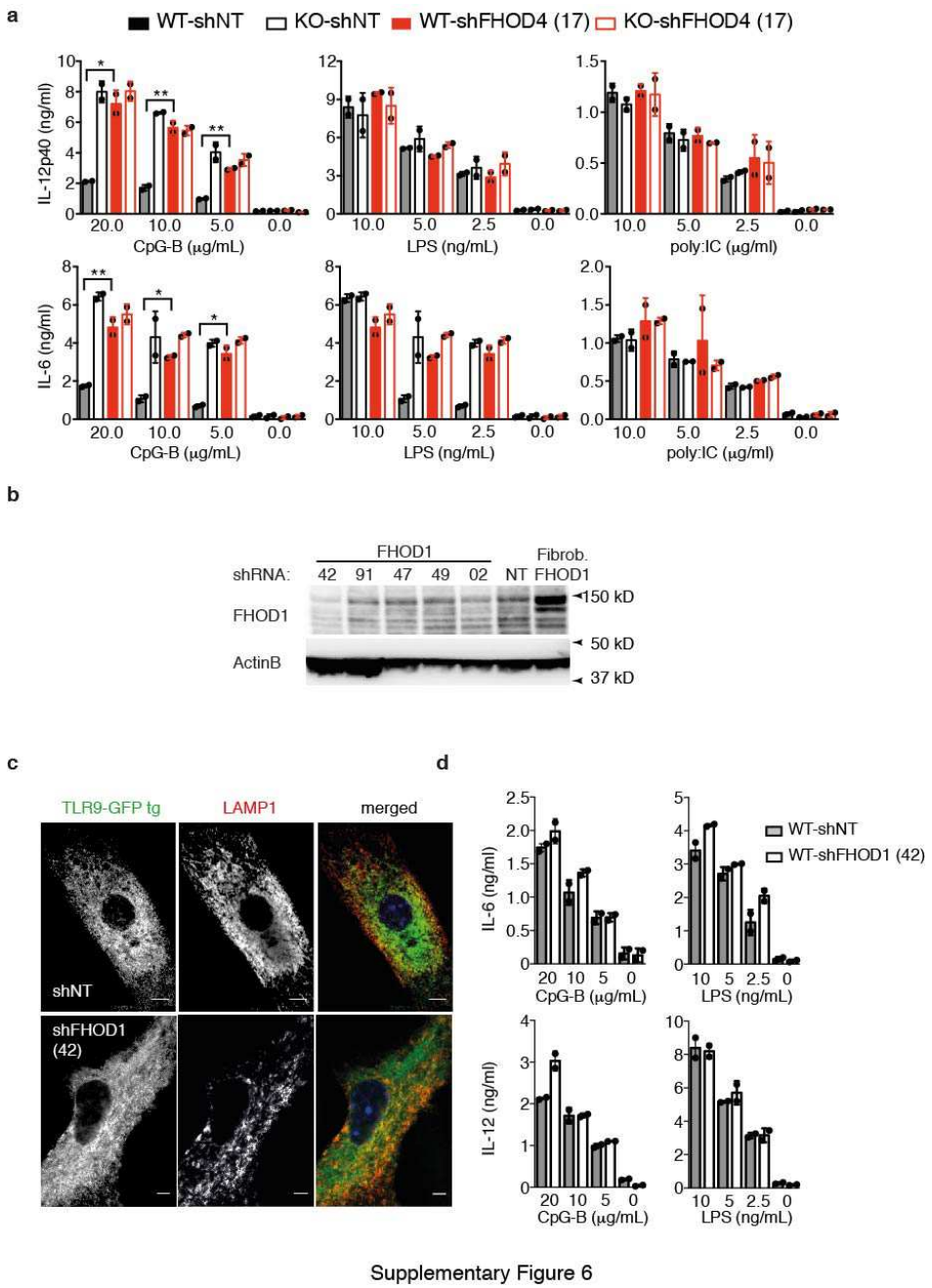

Supplementary Figure 6

Supplementary Figure 6

FHOD4 inactivation, similar to IRAP deficiency, increases TLR9 activation

(**a**) WT and KO BMDCs were transduced with shNT (non-targeting) and shFHOD4 (17) lentiviruses and stimulated with different TLR ligands for 6 h. The secretion of IL-12p40 and IL-6 in supernatants was measured by ELISA (n=2 experiments, mean ± SEM, **p<0.009, *p<0.018). (**b**) BMDCs from TLR9-GFP transgenic mice were transduced with lentiviruses coding for 5 different shRNA against FHOD1 (shFHOD1 42, 91, 47, 49, 02) or a non-targeting shRNA (shNT) and the knock-down efficiency was analyzed by immunoblotting with antibodies specific for FHOD1. WT fibroblasts transfected with a plasmid coding for FHOD1 were used as positive control for anti-FHOD1 antibodies. (**c-d**) BMDCs from TLR9-GFP transgenic mice were transduced with lentiviruses expressing shNT or shFHOD1 (42) and used to analyze TLR9-GFP localization in steady state conditions by confocal microscopy using an anti-LAMP1 antibody (**c**) or to measure the secretion of IL-6 and IL-12(p40) after TLR4 and TLR9 activation (**d**) (n=2 experiments, mean ± SEM).

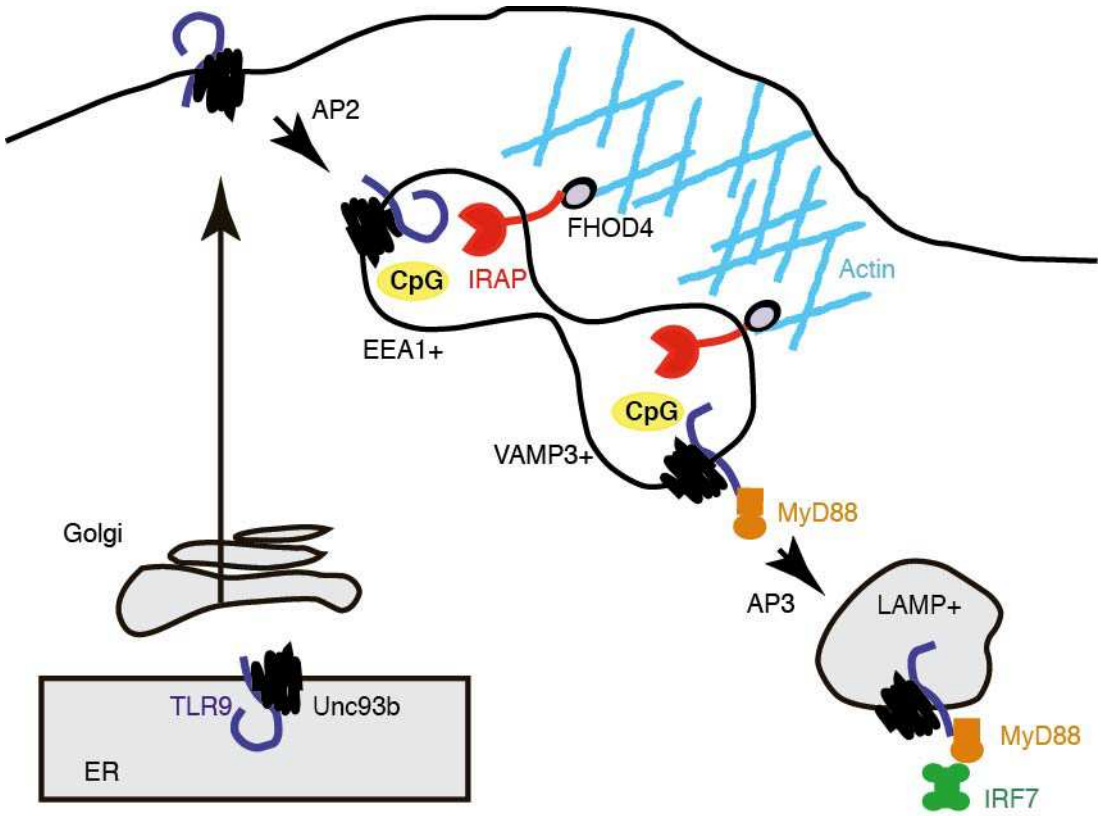

Supplementary Figure 7

Supplementary Figure 7

Integration of literature data and our results for a model of TLR9 trafficking

Under basal conditions, TLR9 is retained in the ER. Upon cell stimulation, the TLR9-Unc93b complex traffics to the cell surface and is internalized via AP2 and clathrin mediated endocytosis [7]. Once intracellular, TLR9 reaches IRAP^{+} endosomes that contain CpG. IRAP vesicles are Rab14 and Stx6 positives and overlap with both EEA1^{+} [8,9] and VAMP3 vesicles. In VAMP3^{+} compartment, TLR9 recruits MyD88 and induces the NF-κB response. The sorting of TLR9 from VAMP3^{+} vesicles is dependent on the clathrin adaptor AP3 [10] and allows TLR9 transport, probably via microtubules [11], to lysosomes, from where it can signal via both, MyD88 and IRFs. Actin polymerization around early endosomal compartments delays CpG and TLR9 transport to lysosomes [12]. IRAP interaction with the actin nucleator FHOD4 anchors the endosomes containing CpG and TLR9 to the actin network, blocking their transport towards lysosomes and limiting TLR9 activation.

Click inside this box and insert a single image for Supplementary Figure 8. For best results, use Insert menu to select a saved file; do not paste images. Source images must be JPEGs (no larger than 10 MB) saved in RBG color profile, at a resolution of 150–300 dpi. Optimize panel arrangement to a 2:3 height-to-width ratio; maximum online display is 600h x 900w pixels. Reduce empty space between panels and around image. Keep each image to a single page.

Delete these instructions before inserting the image.

Supplementary Figure 8

Insert figure title here by deleting or overwriting this text; keep title to a single sentence; use Symbol font for symbols and Greek letters.

Insert figure caption here by deleting or overwriting this text; captions may run to a second page if necessary. To ensure accurate appearance in the published version, please use the Symbol font for all symbols and Greek letters.